Influence of particle size on the ion effect of TiO_2 nanoparticle doped nematic liquid crystal cell

2014 Jpn. J. Appl. Phys. 53 071701

(http://iopscience.iop.org/1347-4065/53/7/071701)

Japanese Journal of Applied Physics **53**, 071701 (2014)
http://dx.doi.org/10.7567/JJAP.53.071701

REGULAR PAPER

Influence of particle size on the ion effect of TiO_2 nanoparticle doped nematic liquid crystal cell

Tsu-Ruey Chou[1], Jung Hsieh[2], Wei-Ting Chen[1], and Chih-Yu Chao[1,2*]

[1]*Department of Physics, National Taiwan University, Taipei 10617, Taiwan*
[2]*Institute of Applied Physics, National Taiwan University, Taipei 10617, Taiwan*
E-mail: cychao@phys.ntu.edu.tw

Received February 20, 2014; accepted May 1, 2014; published online June 23, 2014

In this study, the transient currents of nematic liquid crystal cells doped with different sizes of titanium dioxide (TiO_2) nanoparticles were measured. The experimental results illustrate that doping TiO_2 nanoparticles into nematic liquid crystals leads to a reduction in the moving-ion density and the amount of reduced impurity ions is related to the size of doped TiO_2 nanoparticles. Under the same doping concentration, TiO_2 nanoparticles with a smaller average particle size are more effective in trapping the impurity ions. The measurements of voltage–transmittance curves and time evolution characteristics of the doped liquid crystal cells further confirm this phenomenon. This study suggests that TiO_2 nanoparticles with a smaller size are better candidates as nanodopants for liquid crystal display applications. © 2014 The Japan Society of Applied Physics

1. Introduction

Liquid crystal displays (LCDs) have been developed over 50 years and have become the most dominant product in the display market. Nowadays, LCDs are widely used in our daily life, for example, smart phones, tablet PCs, and large panel televisions. Along with the increasing quality requirements in many technology products, the criteria of LCDs have become more and more rigorous in recent years. In order to achieve high performance displays, researchers have developed several new modes of liquid crystal (LC) devices, such as film-compensated twist-nematic,[1)] in-plane switching,[2)] fringe-field switching,[3)] and multi-domain vertical alignment.[4)] Although each of these LC devices has their unique advantages, there are some common obstacles that should be overcome. One of the most important issues is suppressing the defects caused by impurity ions within the LC device.[5)]

The impurity ions in LC devices originate from the LC material, alignment layer, and sealing glue, etc. Under an applied voltage, ions in the LC host begin to move toward the LC/alignment layer interface and finally are absorbed on the surface of the alignment layer. These absorbed ions form the electric double layer in the LC cell and induce an inner electric field which is opposite to the direction of the applied voltage,[6)] thus leading to an effective voltage reduction in the LC layer. This screening effect results in many defects on the electro-optical properties of the LC device, including the increase in driving voltage, image sticking, flickering, gray-level shift, and voltage holding ratio reduction. In order to overcome these ion-induced problems, the LC mixture employed in the LCD industry must possess a high bulk resistivity and a low ion concentration. Instead of synthesizing high quality LC materials, several methods have been published to reduce the ion effect in LC devices.[7–10)] One of the most effective and feasible way is doping additional materials, especially nanomaterials, into LCs.

Doping nanomaterials into LCs receives great attention these years due to the possibility of showing new characteristics such as dielectric anisotropy enhancement,[11)] memory effect,[12)] frequency modulation,[13)] and low driving voltage.[14)] To date, there are many kinds of nanomaterials used as nanodopants, e.g., conductive nanoparticles,[15)] semiconducting nanoparticles,[16)] insulating nanoparticles,[14,17)] and carbon-related nanomaterials.[18)] The addition of these nanomaterials not only alters the physical and chemical properties of LCs but also enhances the performance of LCDs. It was reported that carbon nanotubes used as a guest dopant could reduce the DC driving voltage and improve the switching behavior of nematic LCs.[19,20)] However, the reorientation of carbon nanotubes after applying a voltage above the Freédricksz threshold degrades the voltage holding ratio of the LC cell,[17)] which restricts the applicability of carbon nanotubes. In recent years, titanium dioxide (TiO_2) nanoparticles have become a considerable material owing to their applications in many electro-optical devices.[21,22)] According to our previous work, the addition of TiO_2 nanoparticles into nematic LCs leads to the reduction of the moving ion-density as well as the threshold voltage while keeping the voltage holding ratio higher than 95%.[23)] We proposed a conceptual depiction of those impurity ions moving in the LC cell and speculate that these ions could be trapped on the surface of doped nanoparticles. Based on our previous result, we consider that, owing to the difference in total surface area of doped nanoparticles, the ion density would perhaps vary with the size of nanoparticles under same doping concentration. In this study, several sizes of TiO_2 nanoparticles were prepared as guest dopants to investigate the relation between the particle size and ion density in nematic LCs. The transient currents and voltage–transmittance (V–T) characteristics of the LC suspensions containing different sizes of TiO_2 nanoparticles have been measured and discussed. The experimental results showed that smaller TiO_2 nanoparticles are more effective in reducing impurity ions within LCs.

2. Experimental methods

TiO_2 nanoparticles were purchased from Nanostructured & Amorphous Materials. The average particle size (APS) of TiO_2 nanoparticles was inspected by means of an FEI Tecnai F20 transmission electron microscope (TEM) operated at 200 kV. A small amount of TiO_2 nanoparticles was dispersed in anhydrous ethanol and dried for about 10 min on the air-plasma-treated copper grid for observation. The empty LC cells were fabricated using two glass substrates coated with indium tin oxide (ITO) and polyimide layer with a 7.5 µm cell gap ensured by spacers. The polyimide layer was rubbed after coating to yield a unidirectional planer alignment and the cell configuration is a 90° twisted nematic (TN) mode. The overlapped area of ITO electrodes was $10 \times 10\,mm^2$.

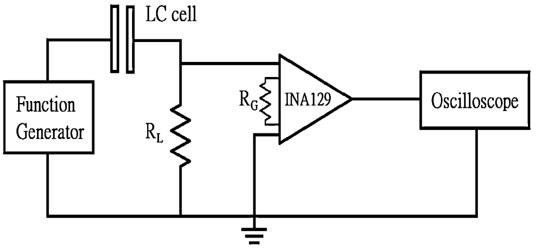

Fig. 1. Experimental setup for the measurement of transient current.

The LC suspensions were prepared by adding TiO_2 nanoparticles of different sizes into nematic LC (E7, Merck) with the same concentration of 0.1 wt%. Each suspension was sonicated for 12 h and then stirred for 1 h to make sure that TiO_2 nanoparticles were uniformly dispersed in LCs. Thereafter, LCs with and without TiO_2 nanoparticles were injected into empty cells by means of capillary action in the isotropic phase. After sample preparation, a polarizing optical microscope (POM) was employed to examine the uniformity of TiO_2 nanoparticle doped LC cells. The schematic setup for transient current measurement is shown in Fig. 1. Each cell was measured by applying a square wave voltage with a frequency of 0.5 Hz and amplitude of 10 V. The resulting leakage current was amplified and measured on the oscilloscope through a series resistor. The applied waveform was repeated about 30 times to reduce the noise by software averaging. The current–voltage characteristic was measured with the same setup by applying a triangular wave voltage with a frequency of 0.02 Hz and amplitude of 10 V. The *V–T* characteristic of each cell from a He–Ne laser source was measured by a silicon photodetector. All cells were placed between a pair of cross-polarizers and measured by applying a triangular wave voltage oscillating between 0 and 10 V with a frequency of 0.02 Hz under the normally white mode. The voltage–capacitance (*V–C*) hysteresis curves were measured by an LCR meter. The DC bias was swept between −10 and 10 V with each step of 0.05 V.

3. Results and discussion

Figures 2(a)–2(c) are TEM images of TiO_2 nanoparticles used in this study. In these micrographs, it can be found that the APS of three different sizes of TiO_2 nanoparticles used in this experiment are uniformly around 5, 10, and 30–40 nm, respectively. The obtained APS values are in accordance with the datasheet of the supplier. The aggregation of nanoparticles in this observation was due to the drying procedure on copper grids. Figures 2(d)–2(f) are the POM images of LC cells doped with 5, 10, and 30–40 nm TiO_2 nanoparticles, respectively. These LC cells were observed under the normally black mode. In the normally black mode, it would be easy to find light leakage spots if there are some texture changes of LC molecules or aggregations of TiO_2 nanoparticles. In these images, it can be found that a uniformly dark state was observed which indicates that the 90° TN configuration was not affected by the doped nanoparticles, and the TiO_2 nanoparticles dispersed well in the LC host.

The transient currents of doped and undoped LC cells are shown in Fig. 3(a). The transient current of nematic LCs induced by polarity-reserved voltage contains three main characteristics: a capacitive charging current and two current peaks. The first peak, originated from the reorientation of the LC molecules, appears within few milliseconds after the polarity of the applied square wave voltage is reversed.[24] This transient current begins to decay and ultimately vanishes after the rotation of LC molecules is stopped. The second peak is caused by the moving ions within the LC layer. When a low frequency square voltage is applied to the cell, ions in the LC host are driven to the surface of the alignment layer. Then, these ions start to move into the opposite side of the cell after the polarity of the applied voltage is changed, which generates the ion current. Because of the trapping effect, not all of these ions are driven immediately. This effect results in ion current enhancement due to more and more trapped ions being removed from the surface of the alignment layer. Finally, the ion current decreases when the amount of ions reaching the opposite side is more than the amount of ions

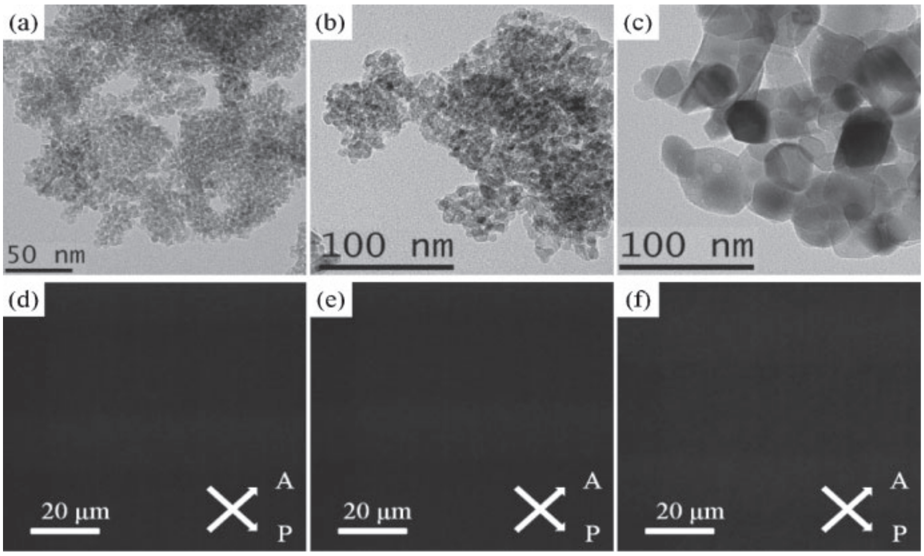

Fig. 2. (a)–(c) TEM images of TiO_2 nanoparticles of three different sizes. The APS values of these TiO_2 nanoparticles are 5, 10, and 30–40 nm, respectively. (d)–(f) POM images of 5, 10, and 30–40 nm TiO_2 nanoparticle doped TN LC cells under normally black mode.

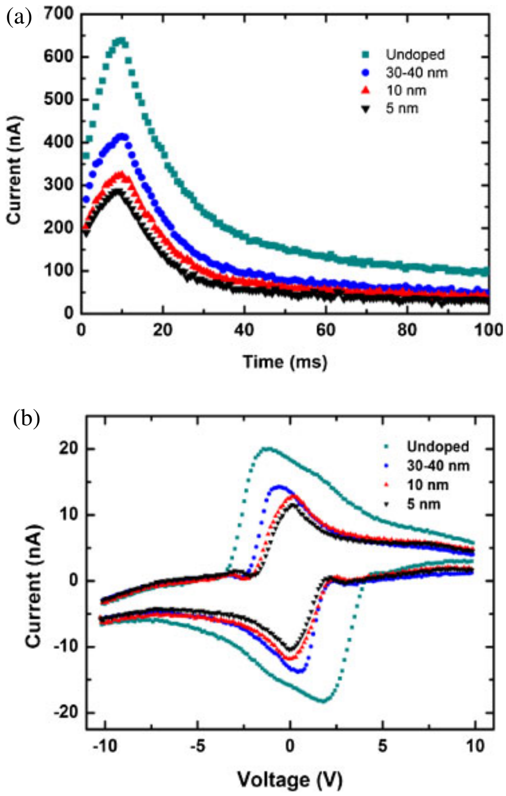

Fig. 3. (Color online) (a) Transient current and (b) current–voltage characteristics of E7 LC and E7 LC doped with different sizes of TiO_2 nanoparticles (0.1 wt%).

removed from the alignment layer. Thus, a current peak is formed. In Fig. 3(a), the current peak at approximately 10 ms of all samples is identified as the second peak induced by moving ions owing to the time of occurrence and the order of magnitude. It is clear that this current bump of the doped LC cells is not only lowered by the addition of TiO_2 nanoparticles compared with the undoped sample but also reduced as the size of TiO_2 nanoparticles decreased. The current peak decreased from 640 nA to 417 nA, 328 nA, and 287 nA for undoped, 30–40 nm-doped, 10 nm-doped, and 5-nm doped samples, respectively. We suggest that the ion concentration of the LC host varies with the particle size of doped TiO_2 nanoparticles, presumably due to the difference in total surface area between the doped nanoparticles with different sizes. Figure 3(b) represents the current–voltage characteristics of doped and undoped samples. The current peaks observed from −2 to 2 V are related to the mobile ions in the LC layer.[25] Similarly, this current peak is suppressed by the doped TiO_2 nanoparticles and the peak value of the cell with smaller nanoparticles is lower than that of the cell with larger nanoparticles. The difference between current peaks of doped samples is conformed to the transient current measurement.

To further investigate the influence of doped particle size on the ion concentration, the *V*–*T* curves of the LC cells were measured. Figures 4(a) and 4(b) are the normalized transmittance of doped and undoped samples measured from the voltage rising part (0 to 10 V) and the voltage falling part (10 to 0 V) of the triangular wave, respectively. The results show that the driving voltage was reduced by the addition of TiO_2 nanoparticles and the amount of voltage reduction increased as the size of doped TiO_2 nanoparticles decreased. This indicates that the LC cells doped with smaller nanoparticles posses lower impurity ions compared with those doped with larger nanoparticles, which confirms the relation of reduced ions and doped nanoparticle size measured by transient current. The threshold voltage, a key factor in LCDs, is defined as the voltage corresponding to 90% of the initial transmittance in this study. The measured threshold voltages from the rising (falling) part of the applied voltage were 6.08 V (7.53 V), 4.35 V (5.77 V), 3.87 V (5.23 V), and 3.77 V (4.94 V) for the undoped, 30–40 nm-doped, 10 nm-doped, and 5 nm-doped samples, respectively. The hysteresis characteristic observed here is due to the trapping effect. Ions driven onto the surface of the alignment layer will not depart from it immediately when the applied voltage decreases, which leads to a higher threshold voltage in the voltage falling part than that of the voltage rising part. This hysteresis phenomenon caused by ions greatly results in gray-level shift which influences the performance of LCDs. Comparing the threshold voltage differences of all samples due to hysteresis, the difference decreased from 1.45 V to 1.42 V, 1.36 V, and 1.17 V for the undoped, 30–40 nm-doped, 10 nm-doped, and 5-nm doped samples, respectively. Furthermore, the hysteresis characteristic was also observed in the *V*–*C* curves, as shown in Fig. 5. The hysteresis width in this measurement is defined as the voltage difference between the rising and falling parts which shows half of the maximum capacity. From Fig. 5, the hysteresis width of doped and undoped LC cells decreased from 3.14 V to 2.73 V, 2.62 V, and 2.48 V for the undoped,

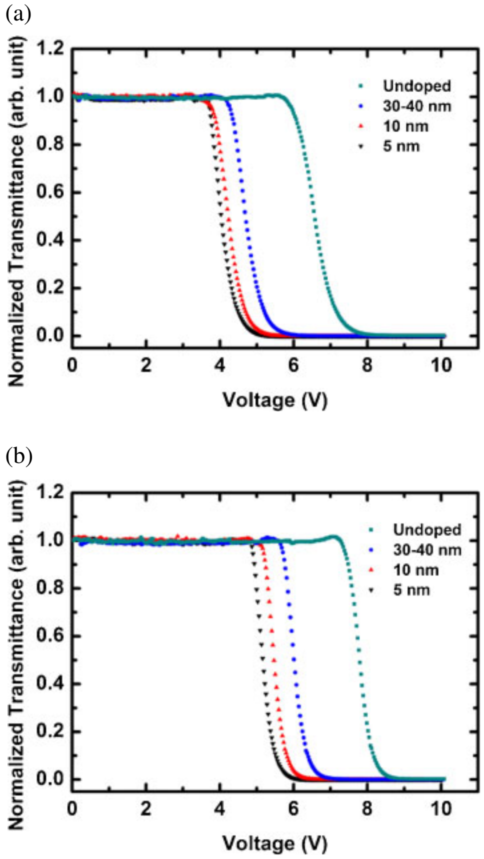

Fig. 4. (Color online) Transmittance of LC cell doped with different sizes of TiO_2 nanoparticles measured by (a) voltage rising part and (b) voltage falling part of a 0.02 Hz 10 V_{pp} triangular wave voltage oscillating between 0 and 10 V.

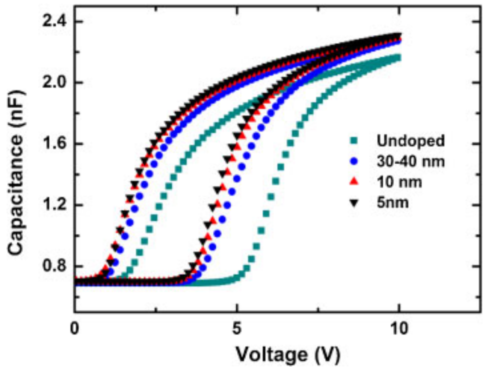

Fig. 5. (Color online) Voltage–capacitance hysteresis curves of E7 LC and E7 LC doped with different sizes of TiO_2 nanoparticles.

30–40 nm-doped, 10 nm-doped, and 5-nm doped samples. The hysteresis width in both V–T and V–C measurements reduced as the size of doped nanoparticles decreased, which is attributed to the lowered ion concentration caused by more ions being adsorbed on smaller nanoparticles.

The Freédricksz threshold voltage for the TN LC cell is given by:

$$V_{\mathrm{th}} = \pi\sqrt{\frac{K_{\mathrm{eff}}}{\varepsilon_0 \Delta\varepsilon}}, \tag{1}$$

where $K_{\mathrm{eff}} = K_{11} + (K_{33} - 2K_{22})/4$ is the effective elastic constant, ε_0 is the permittivity constant of free space, and $\Delta\varepsilon = \varepsilon_{\parallel} - \varepsilon_{\perp}$ is the dielectric anisotropy. In the TN LC cell, the effective elastic constant can be substituted by K_{11} approximately. Previous studies of doping inorganic nanoparticles such as MgO and SiO_2 into nematic LCs stated that the threshold voltage reduction may be attributed to the decrease in the elastic constants.[26] From this point of view, the difference in threshold voltage measured in this study could be ascribed to both the variation of ion density and the elastic constant. However, Walton has shown that the splay (K_{11}) and bend (K_{33}) elastic constants of the TiO_2 nanoparticle doped nematic LCs (up to 0.5 wt %) are similar to those of the undoped LCs.[27] Furthermore, no measurable changes of the threshold voltage were observed under the application of an AC voltage with a frequency of 4 kHz. Therefore, we can conclude that the variation of threshold voltage measured in this study is mainly caused by the difference in ion impurities. In order to investigate the relation between the threshold voltage and ion concentration, threshold voltage drops were calculated from the transient current measurement. The LC cell can be regarded as a capacitor filled with dielectric materials. For simplicity, we neglect the fringing effect because the cell gap is very small compared with the dimension of the ITO electrode. The inner electric field is generated by the ions absorbed on the surface of the alignment layer, therefore, the voltage induced by these ions could be calculated by the formula:

$$V = \frac{\sigma d}{\varepsilon_0 \varepsilon}, \tag{2}$$

where σ is the surface charge density, d is the cell gap, and ε is the dielectric constant of the LC. The surface charge density contributed by ions is determined by integrating the area under the transient current curve. The details of calculating the integration can be found in Ref. 23. The dielectric constant used in our calculation is the dielectric constant parallel to the LC director ($\varepsilon_{\parallel} = 19.0$ for E7) since the applied voltage for measurement is above the Freédricksz threshold. The threshold voltage drops calculated by the difference in surface charge density between undoped samples and doped samples are 1.75, 2.23, and 2.33 V for 30–40 nm-doped, 10 nm-doped, and 5-nm doped samples, respectively. The threshold voltage drop measured from the V–T curves are 1.73, 2.21, and 2.31 V for 30–40 nm-doped, 10 nm-doped, and 5-nm doped samples, respectively. The calculated results are very close to the measured threshold voltage drops, which confirms the relation between the transported ion concentration and the threshold voltage. The slight inaccuracy between the calculated and measured results may originate from the dielectric constant of doped samples which is affected by the doped nanoparticles.

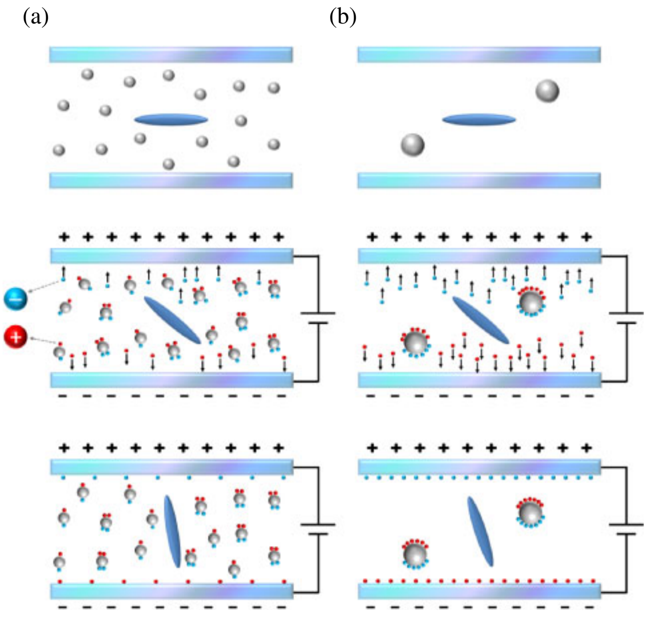

Fig. 6. (Color online) Conceptual depiction of ions behaving in the LC cell doped with (a) smaller size and (b) larger size TiO_2 nanoparticles under the same weight percentage in concentration.

It has been shown that the surface of TiO_2 nanoparticles dispersed in various solutions is charged which attracts those ions in the solution and hence stabilizes the dispersion.[28] Similarly, it could be deduced that some ion impurities in LCs were trapped on the surface of TiO_2 nanoparticles after the doping process. Under an applied voltage, the polarized TiO_2 nanoparticles would change the surface charge distribution and further reduce the ion concentration in LCs. Figure 6(a) is the conceptual depiction of the LC cell doped with smaller TiO_2 nanoparticles and Fig. 6(b) is that for the LC cell doped with larger TiO_2 nanoparticles under the same doping concentration. In both cases, the surface charge (ignored in the figure) and induced dipole moment of TiO_2 nanoparticles can trap ions in the LC host to lessen ion impurities flowing to the surface of the alignment layer and thus suppress the screening effect. In Fig. 6(a), although the surface area of each nanoparticle is less than the surface area of larger nanoparticles, the total surface area of the doped nanoparticles is larger than the total surface area of larger

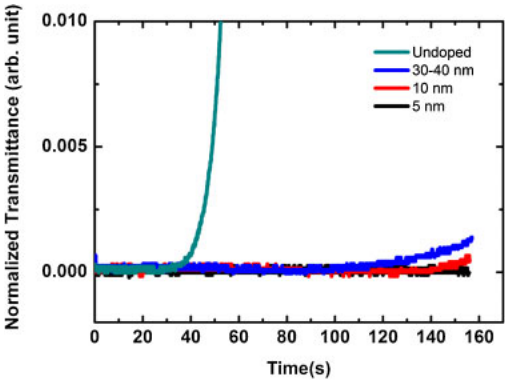

Fig. 7. (Color online) Time-evolved transmittance of E7 LC and E7 LC doped with different sizes of TiO_2 nanoparticles measured by the application of a 10 V DC voltage.

nanoparticles in Fig. 6(b), which leads to more ions being trapped by the nanoparticles and less ions arriving at the alignment layer. Therefore, the ion current and *V–T* curve show that the ion effect in the 5 nm TiO_2 nanoparticle doped cell is less than that in the 10 and 30–40 nm TiO_2 nanoparticle doped cells. The voltage holding ratio (VHR) of the LC cell is defined as the fraction of the voltage maintained over a certain time of the cell after a DC pulse is applied, which is an important parameter of the performance for an active matrix addressed LCD. It has been shown that the VHR value of a high resistance LC material remains nearly the same in the TiO_2 nanoparticle doped samples.[23] In this study, we examined the long-term stability of LC cells by measuring the variation of transmittance under the application of a DC voltage with a relatively long time. When a DC voltage is applied, the transmittance of the cell placed between a pair of cross-polarizers will change gradually due to the accumulated ions on the alignment layer. The more mobile ions in the cell, the more change in the transmittance. The time evolution of the transmittance of doped and undoped LC cells in the normally white mode under a 10 V DC voltage is shown in Fig. 7. The transmittance of all samples decreased to the dark state as the voltage was applied suddenly at 0 s. At 50 s, the transmittance of doped samples is similar to the initial situation while the undoped sample increases to 1% drastically within a short range of time. The applied voltage was fully screened in the undoped sample at about 100 s (not shown in the figure). At 150 s, the transmittance of doped samples increased slightly and the amount of variation increased as the APS of TiO_2 nanoparticles increased, which should be attributed to the difference in ions remaining in the bulk of the LC cell. This result is consistent with the transient current measurement that the sample doped with smaller nanoparticles shows a lower ion concentration compared with the sample doped with larger nanoparticle under the same concentration.

4. Conclusions

In summary, the transient current and the *V–T* characteristic of nematic LCs doped with different sizes of TiO_2 nanoparticles were studied. The transient current measurement shows that the amount of reduced ions increased as the size of doped TiO_2 nanoparticles decreased, which indicates that the LCs doped with smaller TiO_2 nanoparticles posses lower ion impurities. The threshold voltage and hysteresis width measurements from *V–T* curves further confirm that LCs doped with smaller TiO_2 nanoparticles suffer less screening effect caused by ions. The relation between the transported ion density and the threshold voltage is confirmed by comparing the calculated and measured threshold voltage reductions. We suggest that the surface charge and induced dipole moment of TiO_2 nanoparticles could physically trap the ions on their surfaces by Coulomb force. Therefore, the ion concentration of the LC host varies with the size of TiO_2 nanoparticles due to the difference in total surface area of the guest dopant. This study suggests that smaller nanoparticles are better candidates for one to use in order to suppress the unwanted ion effects in LCDs.

Acknowledgments

One of the authors (CYC) would like to thank National Taiwan University, National Science Council, and Ministry of Education of the Republic of China for financial supports on this work.

---

1) J. Chen, K. H. Kim, J. J. Jyu, J. H. Souk, J. R. Kelly, and P. J. Bos, SID Symp. Dig. Tech. Pap. **29**, 315 (1998).
2) M. Oh-e and K. Kondo, Appl. Phys. Lett. **67**, 3895 (1995).
3) S. H. Lee, S. L. Lee, and H. Y. Kim, Appl. Phys. Lett. **73**, 2881 (1998).
4) A. Takeda, S. Kataoka, T. Sasaki, H. Chida, H. Tsuda, K. Ohmuro, T. Sasabayashi, Y. Koike, and K. Okamoto, SID Symp. Dig. Tech. Pap. **29**, 1077 (1998).
5) S. H. Perlmutter, D. Doroski, and G. Moddel, Appl. Phys. Lett. **69**, 1182 (1996).
6) H. Mada and K. Osajima, J. Appl. Phys. **60**, 3111 (1986).
7) Y. J. Lim, I. H. Jeong, H. S. Kang, S. Kundu, M. H. Lee, and S. H. Lee, Appl. Phys. Express **5**, 081701 (2012).
8) S. W. Liao, C. T. Hsieh, C. C. Kuo, and C. Y. Huang, Appl. Phys. Lett. **101**, 161906 (2012).
9) Y. Huang, P. J. Bos, and A. Bhowmik, J. Appl. Phys. **108**, 064502 (2010).
10) K. Furuichi, J. Xu, M. Inoue, H. Furuta, N. Yoshida, A. Tounai, Y. Tanaka, A. Mochizuki, and S. Kobayashi, Jpn. J. Appl. Phys. **42**, 4411 (2003).
11) A. Glushchenko, C. Il Cheon, J. West, F. H. Li, E. Buyuktanir, Y. Reznikov, and A. Buchnev, Mol. Cryst. Liq. Cryst. **453**, 227 (2006).
12) A. Glushchenko, H. Kresse, G. Puchkovs'ka, V. Reshetnyak, Y. Reznikov, and O. Yaroshchuk, Mol. Cryst. Liq. Cryst. **321**, 15 (1998).
13) Y. Shiraishi, N. Toshima, K. Maeda, H. Yoshikawa, J. Xu, and S. Kobayashi, Appl. Phys. Lett. **81**, 2845 (2002).
14) F. Haraguchi, K. I. Inoue, N. Toshima, S. Kobayashi, and K. Takatoh, Jpn. J. Appl. Phys. **46**, L796 (2007).
15) H. Yoshida, Y. Tanaka, K. Kawamoto, H. Kubo, T. Tsuda, A. Fujii, S. Kuwabata, H. Kikuchi, and M. Ozaki, Appl. Phys. Express **2**, 121501 (2009).
16) T. Zhang, C. Zhong, and J. Xu, Jpn. J. Appl. Phys. **48**, 055002 (2009).
17) P. S. Chen, C. C. Huang, Y. W. Liu, and C. Y. Chao, Appl. Phys. Lett. **90**, 211111 (2007).
18) M. Suzuki, H. Furue, and S. Kobayashi, Mol. Cryst. Liq. Cryst. **368**, 191 (2001).
19) W. Lee, C. Y. Wang, and Y. C. Shih, Appl. Phys. Lett. **85**, 513 (2004).
20) I. Dierking, G. Scalia, and P. Morales, J. Appl. Phys. **97**, 044309 (2005).
21) W. K. Lee, J. H. Choi, H. J. Na, J. H. Lim, J. M. Han, J. Y. Hwang, and D. S. Seo, Opt. Lett. **34**, 3653 (2009).
22) Y. M. Chang, W. F. Su, and L. Y. Wang, Macromol. Rapid Commun. **29**, 1303 (2008).
23) W. T. Chen, P. S. Chen, and C. Y. Chao, Jpn. J. Appl. Phys. **48**, 015006 (2009).
24) H. Naito, K. Yoshida, M. Okuda, and A. Sugimura, J. Appl. Phys. **73**, 1119 (1993).
25) K. Ono and J. Nakanowatari, Jpn. J. Appl. Phys. **30**, 2832 (1991).
26) S. Kobayashi, Y. Saeki, S. Kodaira, K. Takatoh, T. Kineri, H. Hoshi, N. Toshoma, and S. Sano, J. Soc. Inf. Disp. **16**, 871 (2008).
27) H. G. Walton, Mol. Cryst. Liq. Cryst. **574**, 60 (2013).
28) A. Fernández-Nieves and F. J. de las Nieves, Colloids Surf. A **148**, 231 (1999).